Microtrenching resulting from specular reflection during chlorine etching of silicon

Robert J. Hoekstra[a] and Mark J. Kushner[b]
Department of Electrical and Computer Engineering, University of Illinois, 1406 W. Green St., Urbana, Illinois 61801

Valeriy Sukharev and Phillipe Schoenborn
LSI Logic Corporation, 3115 Alfred St., Santa Clara, California 95054

(Received 9 February 1998; accepted 10 April 1998)

In an effort to increase throughput, the microelectronics fabrication industry has transitioned to high plasma density etching reactors using large source (>800 W) and moderate substrate bias (>100 W) powers in which the ion to neutral radical flux is large compared to reactive-ion-etching systems. These conditions can lead to microtrenching where etch rates are largest at the base of the sidewalls. Microtrenching has been attributed to specular reflection of high energy particles, usually ions, at grazing angles on the sidewalls of the mask and trench. These reflections produce a ''focusing'' of flux to the corners of the trench which results in locally enhanced etching. In this letter, integrated plasma equipment and Monte Carlo feature profile models have been used to examine the processes and conditions which produce focused fluxes and microtrenching, including the degree of specular reflection and sidewall slope of the mask. Quantitative comparisons are made to experimental measurements of etch profiles. © *1998 American Vacuum Society.*
[S0734-211X(98)00804-X]

As the feature sizes of microelectronics devices decrease to sub-0.5 μm dimensions, the semiconductor fabrication industry is increasingly employing dry etching techniques using high plasma density reactors such as inductively coupled plasma (ICP) systems.[1] These tools differ from conventional reactive-ion-etching (RIE) reactors in that the ratio of the ion flux to the reactive neutral flux to the substrate is larger. Microtrenching is one possible consequence of these conditions. Microtrenching refers to profiles for which the etch rate is larger near the corners of a trench compared to the center of the trench. The etch profile across the floor of the trench is therefore either convex or has vertical slots at the base of the sidewalls. Microtrenching is believed to be produced by the impact of high energy particles (mostly ions) at grazing angles ($>80°$) on the sidewalls followed by specular reflection where the particles retain a large fraction of their energy and directionality. These conditions lead to ''focusing'' of the high energy particles at the base of the sidewalls of the feature, resulting in higher etch rates at those locations. Microtrenching can lead to large differences in etch depth across the bottom of features and the possibility of ''punchthrough'' on etch stops or other thin layers such as gate oxide. Microtrenching was first discussed by Nguyen *et al.*,[2] and the proposal that specular reflection is a major contributing cause was first made by Dalton *et al.*[3]

As plasma equipment models and profile simulators have matured, the ability to self-consistently predict the consequences of plasma-surface interactions on etch profiles has also significantly improved.[4–7] In this regard, in this letter we present results from integrated plasma equipment and profile models to investigate the consequences of specular reflection by high energy grazing-angle ions and neutrals on profile evolution during chlorine plasma etching of Si. The plasma simulator we used in this study is the hybrid plasma equipment model (HPEM) and the profile simulator is the Monte Carlo feature profile model (MCFPM). The models, and their method of integration, are described in Refs. 4 and 8. In the MCFPM, the trench is resolved in two dimensions using a rectilinear numerical mesh having 500×500 cells for a $1\ \mu\text{m}\times1\ \mu$m region. Computational particles are directed towards the surface representing the energy and angularly resolved ion and neutral fluxes produced by the HPEM. Monte Carlo techniques are applied to changed the identity of a mesh cell to represent, for example, adsorption, passivation, and etching processes. The reaction mechanism we used is based on successive chlorination of Si by neutral Cl atoms followed by ion stimulated desorption of $SiCl_n$.[4]

The MCFPM differs from that previously described in the method of treating ion (or high energy neutral) reflections from surfaces. Due to the statistically rough surface inherent to Monte Carlo based simulators, it is necessary to locally smooth the surface at the site of impact to eliminate unrealistic high angle scattering from sharp boundaries of the numerical mesh between the surface and plasma. This smoothing was accomplished by sampling the actual plasma-surface boundary 10–20 cells on either side of the point of impact and making a least-squares fit to the surface. The incident particle then collides and reflects from the smoothed surface.

All experimental and model results discussed in this article are for an inductively coupled LAM 9400SC plasma etching reactor.[9] The reactor operating parameters are: 600 W inductively coupled power, 100 W substrate bias at 13.56 MHz, and 10 mTorr of Cl_2 at a flow rate of 60 sccm. The

[a]Electronic mail: stretch@uigela.ece.uiuc.edu
[b]Electronic mail: mjk@uiuc.edu

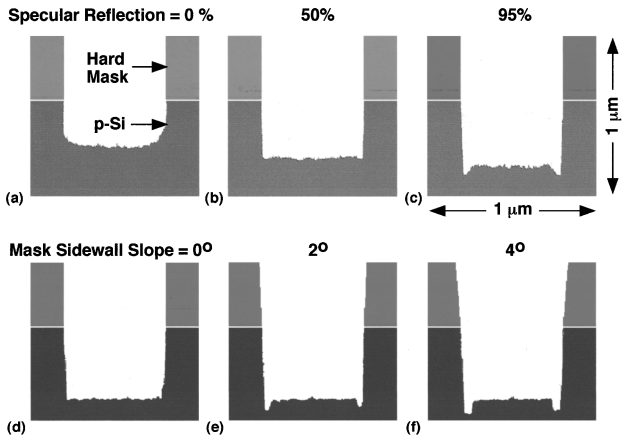

FIG. 1. Etch profiles for chlorine etching of silicon for (a) 0%, (b) 50%, and (c) 95% specular reflection and for outward slope of the mask sidewalls of (d) 0°, (e) 2°, and (f) 4°.

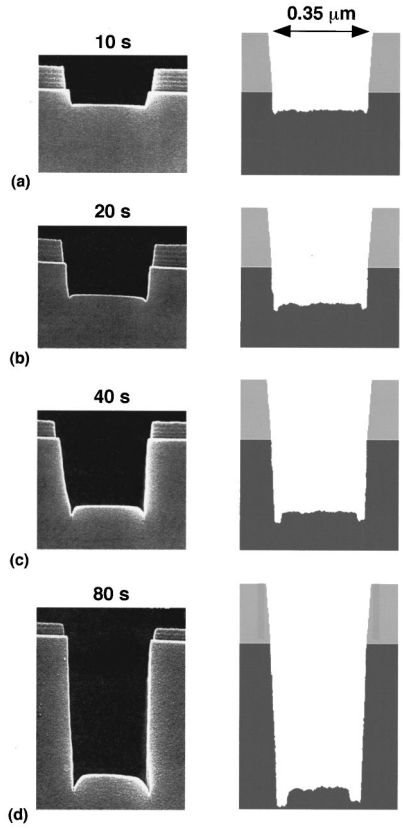

FIG. 2. Comparison of experimental etch profiles (left-hand side) and results from the model (right-hand side) for etch times of (a) 10, (b) 20, (c) 40, and (d) 80 s.

system we are addressing is etching of crystalline Si using a hard mask of SiO_2. The angular dependence of the etch yield of chlorine atomic ions on silicon we used in the MCFPM is that measured by Chang and Sawin.[10] We specified that ions retain as much as 99% of their energy when reflecting at grazing angles ($>80°$) based on results from molecular dynamics simulations by Helmer and Graves.[11] We ignored the effects of surface charging on ion trajectories in the trench due to the moderately high conductivity of the substrate, though charging in the trench is an important process in producing notching.[12]

To demonstrate the dependence of microtrenching on the degree of specular reflection (SR), the fraction of grazing ions allowed to retain their energy was varied from 0% to 95%. The resulting profiles, shown in Figs. 1(a)–1(c) for 0.6 μm wide trenches, reveal significant changes in the morphology of the bottom of the trench. As the fraction of SR is increased, the corners of the trench evolve from being rounded at 0% SR, to being sharp and square at 50%, and finally to having microtrenches at the base of the sidewalls at 95% SR. The onset of microtrenching is a direct result of ion reflection from the sidewalls leading to ''focusing'' or enhancement of the particle flux at the base of the sidewall. The increased particle flux produces a higher etch rate which, if sufficiently focused, generates microtrenching, generally at SR$>$90%.

The slope of the sidewall of the mask can also play an important role in the initial development of microtrenching. A finite slope of the mask increases the solid angle of the ion flux from the plasma that can reflect from its sidewalls. Since the angular spreads of the ion flux for the conditions of interest are typically $<4°-5°$, a small variation in the slope of the mask sidewall accesses a significantly larger fraction of the ion flux. For example, the etch profiles shown in Figs. 1(d)–1(f) were obtained by varying the slope of the mask sidewalls from 0° to 4°. As the slope is increased the microtrenching becomes more pronounced and broader. Note that as the depth of the trench increases the relative area of the mask sidewall decreases compared to the exposed sidewall of the trench. Therefore the influence of the slope of the mask on microtrenching is less pronounced for deeper trenches. However, since the solid angle of the ion flux accessible by the sidewalls of the mask is always larger than that for the trench, its slope is always an important consideration.

The evolution of microtrenching is shown in Fig. 2 where predictions from the simulation are compared to experimental results for 0.35 μm wide trenches at different times during the etch. A 0.2 μm thick hard mask was used in the model, while a 0.1 μm hard mask was used experimentally which etched at a rate approximately 5% that of the silicon. The predicted and experimental profiles show the same trends. As the trench deepens, the depth and width of the microtrenches increases as more sidewall area is available to reflect and focus ions. The model shows a more severe broadening of the microtrenches than found in the experiments which may be a consequence of the discreteness of the numerical mesh.

The angular dependence of sputtering yield is typically depressed at normal incidence with a maximum near 60° as recently demonstrated by molecular dynamics simulations by Hanson *et al.*[13] for the sputter yield of Cl^+ on Si. Experiments by Chang and Sawin,[10] however, show a broad maximum in the etch yield of Cl^+ on Si from 0° to 40° with a gradual decrease approaching 90°. These results indicate that

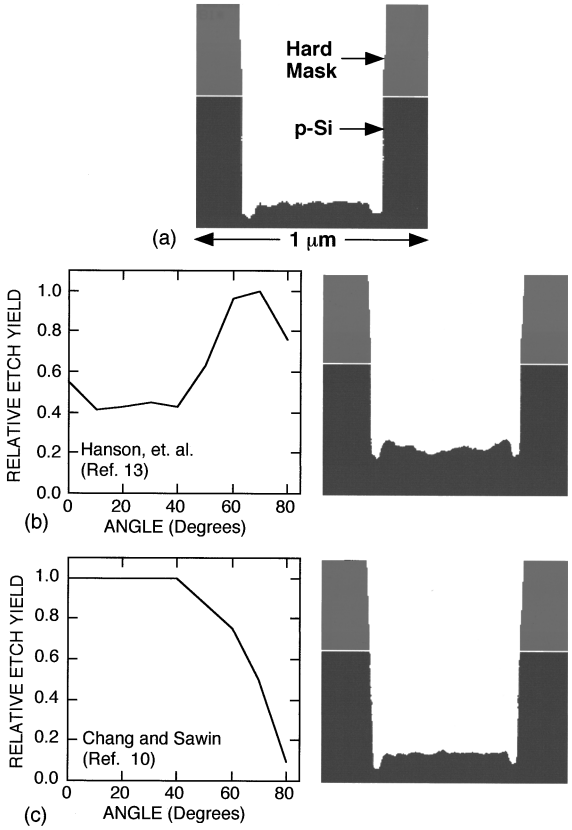

FIG. 3. Etch profiles for different models of the angular dependence of etch yield. (a) Uniform angular dependence, (b) angular dependence as given by Hanson *et al.* (Ref. 13), shown at left for 100 eV ions, (c) angular dependence as given by Chang and Sawin (Ref. 10), shown at left for 35 eV ions.

the mechanism for ion enhanced etching may differ from simple sputtering. The precise forms of these etch yields do have an influence on microtrenching. These trends are shown in Fig. 3 where profiles are plotted for the same etch times while using different angular dependencies for the etch yield. The slope of the mask sidewall is 2°. The profile in Fig. 3(a), the base case, was obtained with no angular dependence of the etch yield. The sidewalls of the trench have a shallow angle and the microtrench is broad due to there being a broad angular flux of reflected ions. The profile in Fig. 3(b) was obtained using the angular dependence of Hanson *et al.* The etch rate is smaller than for the base case since the relative etch yield at near normal incidence is lower. The sidewalls are nearly vertical due to the larger etch yield at grazing angles. There is also structure on the floor of the trench resulting from the extrema in the etch yield and energy loss of ions reflecting from the walls. The profile generated using the etch yields from Chang and Sawin [Fig. 3(c)], has narrower microtrenches than the base case, due to there being fewer losses of grazing incidence ions on the sidewalls. The sidewall slope is larger than for the yields of Hanson *et al.* due to the decrease in etch yield at grazing angles. The total etch rate is commensurate with the base case due to the larger yield at normal angles.

In conclusion, a Monte Carlo feature profile model has been used to investigate the effects of specular reflection of grazing-angle ions on the profile evolution and microtrenching in chlorine plasma etching of silicon. We found that the SR of ions from the sidewalls must exceed 90% at grazing incidence ($>80°$) to reproduce experimentally observed microtrenching. The slope of the sidewall of the mask also has an important influence on microtrenching. Sidewall slopes of 2°–4°, commensurate with the angular spread of the incoming ion flux, increases microtrenching by accessing a larger solid angle of the ions. The angular dependence of the etch yield influences microtrenching as well. Low yields at high angles of incidence allow more ions to retain a larger fraction of their energy after reflection from the sidewalls, thereby producing a narrower microtrench. Microtrenching increases with increasing etch depth due to the larger sidewall area available for ion reflection.

This work was supported by the Semiconductor Research Corporation, National Science Foundation (ECS 94-04133, CTS 94-12565), and the University of Wisconsin ERC for Plasma Aided Manufacturing.

[1]J. H. Keller, Plasma Sources Sci. Technol. **5**, 166 (1996).
[2]S. V. Nguyen, D. Dobuzinsky, S. Stiffler, and G. Chrisman, J. Electrochem. Soc. **138**, 1112 (1991).
[3]T. J. Dalton, J. C. Arnold, H. H. Sawin, S. Swan, and D. Corliss, J. Electrochem. Soc. **140**, 2395 (1993).
[4]R. J. Hoekstra, M. J. Grapperhaus, and M. J. Kushner, J. Vac. Sci. Technol. A **15**, 1913 (1997).
[5]V. Singh, E. S. G. Shaqfeh, and J. P. McVittie, J. Vac. Sci. Technol. B **12**, 2952 (1994).
[6]B. Abraham-Shrauner and W. Chen, J. Vac. Sci. Technol. B **14**, 3492 (1997).
[7]N. Hamaguchi and S. M. Rossnagel, J. Vac. Sci. Technol. B **13**, 183 (1995).
[8]M. J. Grapperhaus and M. J. Kushner, J. Appl. Phys. **81**, 569 (1997).
[9]LAM Research Corp., Fremont, CA; URL http://www.lamrc.com
[10]J. Chang and H. H. Sawin, J. Vac. Sci. Technol. A **15**, 610 (1997).
[11]B. A. Helmer and D. B. Graves, presented at the 44th Annual Symposium of the American Vacuum Society, San Jose, CA, October 1997, paper PS-ThA10.
[12]G. S. Hwang and K. P. Giapis, J. Vac. Sci. Technol. B **15**, 70 (1997).
[13]D. E. Hanson, A. F. Voter, and J. D. Kress, J. Appl. Phys. **82**, 3552 (1997).